



Energy Efficiency Performance in Green Residential Building Through Sensitivity Analysis of Biogeography-Based Optimization

Ravinder Kumar¹, Hanumant Pandurang Jagtap²

1. Director Research, Karnavati University, Gandhinagar-382422, Gujarat, India

2. Assistant Professor, Zeal College of Engineering and Research Narhe, Pune-411041, Maharashtra, India

Article Info

Received [\[\]](#)

Received in Revised form [\[\]](#)

Accepted [\[\]](#)

Published online [\[\]](#)

DOI: [\[\]](#)

Keywords

Cooling-load

Residential buildings

Computational Intelligence,

BBO

Hybrid

Abstract

We utilized the most applicable artificial intelligence systems for the challenge of cooling load (CL) in housing units. We fine-tuned them in 2 stages using an innovative evolutionary algorithm called Biogeography-Based Optimization (BBO). The abovementioned procedure is then applied to establish a connection between the system's input and output characteristics. The vital output of the system was the measure of CL. In contrast, the input attributes included surface area, relative compactness, roof area, wall area, glazing area distribution, overall height, and orientation. Two well-known statistical indices, the correlation coefficient (R^2) and root mean squared error (RMSE) were used to assess the BBO approach's expected outcome for data sets. According to the findings of the BBO network's initial stage, the R^2 and RMSE amounts for the training and testing data sets were 0.965281 and 0.06773, respectively. Per the R^2 and RMSE, the testing data set, and suggested BBO-MLP forecasting network models acquired amounts of 0.96007 and 0.06946, respectively. In the second stage, data are collected for ten distinct alpha values. These data suggest that an alpha of 1.1 provides excellent efficiency. In addition, the amounts of R^2 and RMSE for the testing data set is (0.95113 and 0.07667) and (0.95574 and 0.07628) for the training data set, respectively.

1. Introduction

Today's world has witnessed the insatiable desire of emerging countries to achieve developed nation status. In attaining such, many nations overlook the need for renewable energy and lowering carbon emissions [1]. The government has turned to extensive building restorations and replacements to accommodate the population's necessities, such as housing. Research has shown that faulty housing structures and designs resulting from rushed planning account for 40 percent of carbon dioxide emissions [2]. Inadequate time and space restrictions to complete the specified construction project resulted in an unsuitable building design, propelling India to fourth place in CO₂ emissions. [GHG statistics from UNFCCC (United Nations Framework Convention on Climate Change)]. Therefore, it is now even more crucial to take action to limit this quantity. This research aims to address this issue

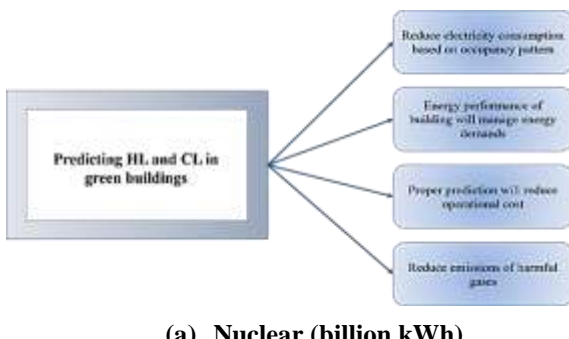
by leveraging the buildings' energy performance (EPB) to reduce their energy usage. This topic has garnered much scholarly attention in recent years [3]. Efforts to enhance the EPB might alleviate this dire circumstance.

Therefore, estimating cooling load based on fundamental characteristics of buildings, including wall area, surface area, and overall height, might assist in determining EPB [4]. Such techniques are prevalent even in HVAC projects [5]. Estimating cooling demand may also aid in reducing building power use and lowering CO₂ emissions [6, 7]. Research has also shown a clear association between energy usage and CO₂ emissions in Nigeria [8], demonstrating that the proposed assumption applies to other countries besides Nigeria. The researchers [9] evaluated the energy-saving potential and discovered that building occupancy and design are the two most



Corresponding author: rav.chauhan@yahoo.co.in (Ravinder Kumar)

essential aspects strongly associated with EPB. Gul and Patidar's [10] research on energy usage verifies Chung and Rhee's [9] research study, which highlights that these guidelines are relevant not just in Korea but in many other parts of the globe, emphasizing the importance of building design in conserving energy. Thus, we can infer that forecasting cooling load will also enable us to define the structure of a refurbished building. Still, it would also allow us to lower the building's energy usage based on its occupancy pattern and create intelligent buildings [11-14]. Figure 1 highlights the necessity of forecasting the cooling demand in buildings.



(a) Nuclear (billion kWh)

Figure 1. Importance of the forecast of heating and cooling loads in green buildings

Scholars such as Yang et al. [15], Li and Li [16], Deb et al. [17], and Malkawi et al. [18] have become increasingly interested in estimating power usage in building structures. According to Lechtenbohmer and Schürer, housing areas have a substantial influence on natural resources [19]. Consequently, these structures prepare facilities for human needs, and their numerous contributions to the community cannot be ignored. Moreover, some scholars argue that construction has harmed the environment over the past few decades [16]. Metals, hydrocarbons, and electrical energy form the basis of the modern world's industrial process. These are interconnected; one is controllable if sufficient energy is available to generate the others. World energy usage in 2013 was around 12,928.4 million tonnes [20]. In 2008, the world energy usage was around 474 Exajoules (EJ), most of which was provided by fossil fuels. In addition, global power usage increased by 70 percent from 1990 to 2008 [20]. Building accounts for around 40 percent of global power consumption and plays a significant role in the energy industry, accounting for approximately 30 percent of global CO₂ emissions.

Furthermore, Madadnia et al. [21] and Ahmad et al. [22] reported that the building's HVAC system

meets its cooling demands. Sensors and automated machines are often used to calculate the cooling load. However, modern commercial building management systems (BMSs) may not always accurately estimate the cooling demand of a structure. Therefore, predicting cooling load and energy usage is challenging due to the numerous interdependent elements involved, such as the wide range of appliances and modifications to buildings to meet the growing population's needs [23, 24]. The need for an excellent alternative to load prediction remains, and more reliable prediction models must be developed to assist engineers and scientists in assessing sustainability challenges throughout the building construction stage. Tsanas and Xifara's writings include references to HVAC regulations [25]. Their technique used simulations that created twelve distinct building forms. The HVAC system serves as the stimulus for managing the indoor climate. Consequently, expecting a cooling load saves energy. Numerous hours have been devoted to anticipating the building cooling demands. Various machine learning approaches have been effectively used to predict the cooling of buildings. Deb et al. [17] have implemented an artificial neural network.

In instances when even non-linear hypotheses fail to learn, ANN is commonly employed. Khayatian et al. [26] also predicted energy performance using the ANN. Yang et al. [15] have used LS-SVM (Least Squares Support Vector Machine) and evaluated SVM against ANN, which employs a backpropagation technique to learn, by utilizing LS-SVM. Yang et al. [15] demonstrated that SVM outperforms ANN in terms of decreasing R-squared and MAPE. Yu et al. have employed hierarchical multi-class SVDD and attained high precision in their study [27]. Roy et al. [28] also experimented with an extreme learning machine, a multivariate adaptive regression spline, and a hybrid approach combining ELM and MARS prediction models. Their outcomes were quite remarkable.

This research proposes four models that forecast the cooling demand of residential structures as a response to the pressing need for energy conservation. The forecast of cooling demand is advantageous in several respects; for instance, it enables designers to make informed decisions about a building's sustainability. Forecasting approaches for loads may also be employed to create buildings with higher energy efficiency.

2. Established database

Tsanas and Xifara [25] utilized the computer program Ecotect [29] to model the CL of twelve residential structures. Concerning 12 researched building structures (with 18 components in a 771.75 m³ volume), four orientations, four glazing regions (0 percent, 10 percent, 25 percent, and 40 percent of the floor area), and five allocation situations, namely uniform (25 percent glazing on each side), South (55 percent on the South and 15 percent on each other side), North (55 percent on the North and 15 percent on each other side), and East (55 percent on the East and 15 percent on each other side) were examined (Figures 2). The variations of the utilized database with the cooling load are shown in Figure 3. Similar research, such as [25, 30], provides further information regarding the dataset utilized.

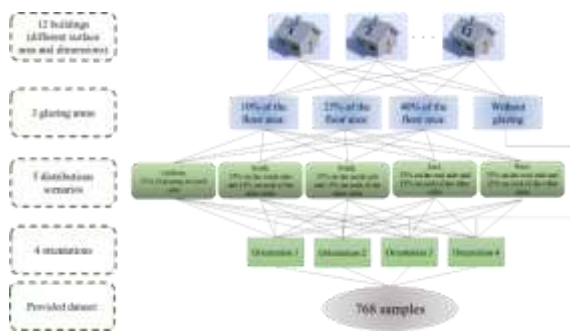
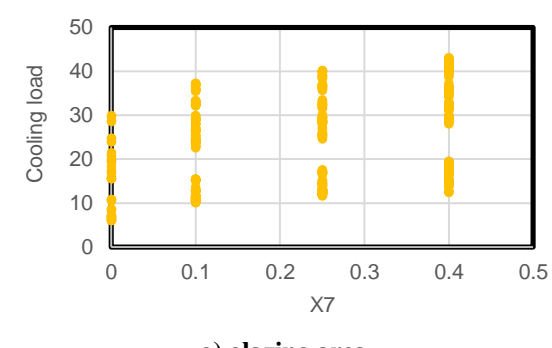
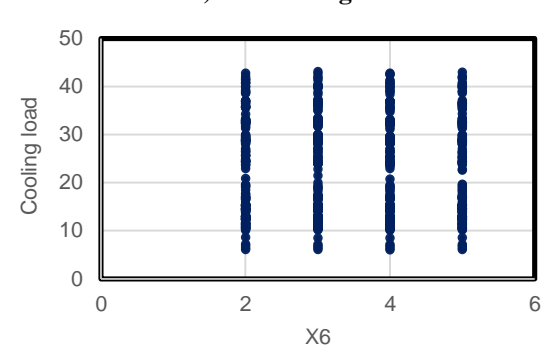
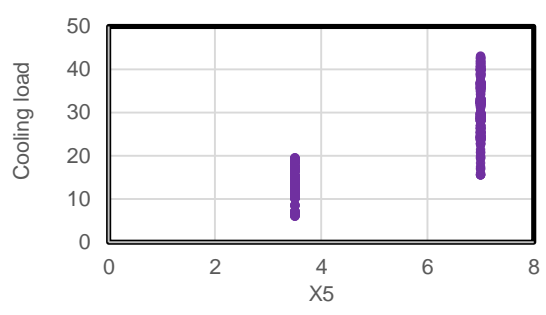
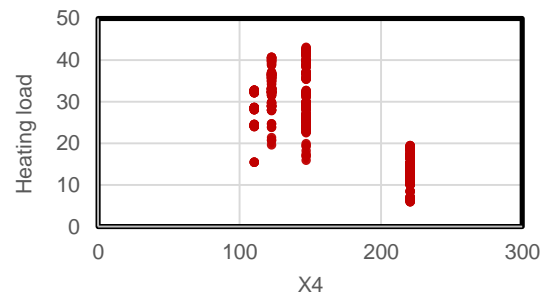
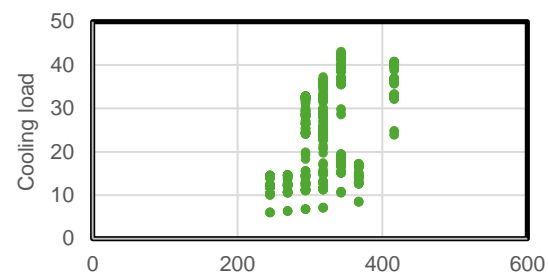
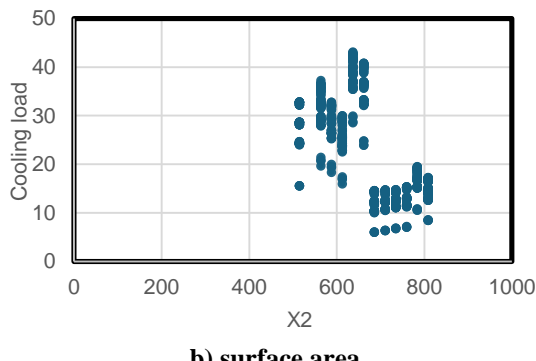
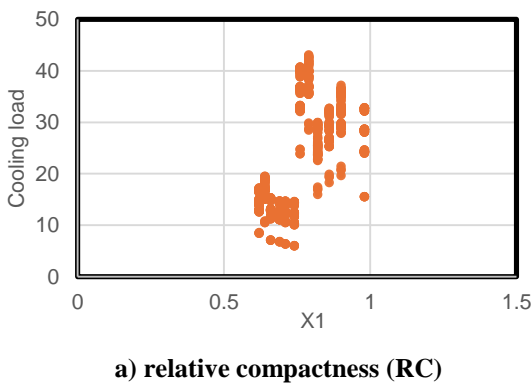
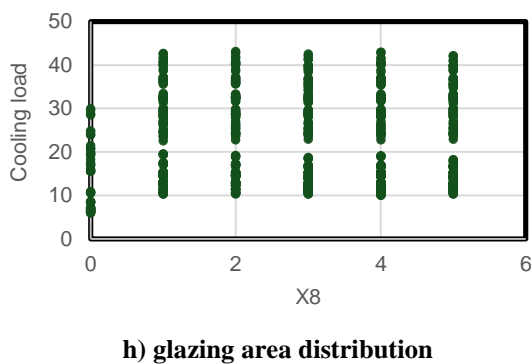


Figure 2: Graphical view of data preparation





h) glazing area distribution

Figure 3: Schematic view of variations of the utilized database with the cooling load

3. Methodology

The general methodology used to achieve the goal of this research (i.e., the subsequent actions) is as follows:

- Data preparation involves arbitrarily dividing the input database into testing and training sets. Eighty percent of it is utilized to feed the approaches that determine the link between the CL and its relevant components, as is well-established.
- Using the MATLAB 2014 programming language, the optimal structure of the MLP neural network is determined, and it is provided quantitatively to the suggested BBO algorithm to identify the optimal solution to the issue. The output is generated through a trial-and-error procedure to determine the optimal variables of the model. The optimization procedure is then performed, and the output is acquired.
- Utilizing the other 20% of the data, the efficiency failure of the approaches is evaluated by employing two widely applied error criteria: root mean square error (RMSE) and mean absolute error (MAE). In addition, the determination coefficient measures the correlation of the findings (R^2).

3.1 Multilayer perceptron:

MLP neural networks are composed of layered units [31]. Each layer consists of nodes, and each node is linked to every node in the layer below it. At least three layers comprise each MLP, including an output layer, one or more hidden layers, and an input layer. Inputs are distributed to successive levels via the input layer. Input nodes are equipped with linear activation functions and lack limits. In addition to weights, every output node and hidden node has limitations. The secret

unit nodes' activation functions are non-linear, but the outputs' activation functions are linear.

Consequently, each signal entering an anode in a successive layer multiplies the original input by a weight and applies a limit before passing through a linear or non-linear activation function (in hidden units). Figure 4 illustrates a typical three-layer network of this kind. In this study, only three-layer MLPs will be investigated, as it has been demonstrated that such networks can simulate any continuous function [32-34]. All inputs and outputs are directly linked to the real three-layer MLP [31].

The training data are a collection of NV training patterns of the form (x_p, t_p) , where P is the pattern index. XP represents the Pth training pattern's N-dimensional input vector, and YP represents the trained network's M-dimensional output vector for the Pth training pattern. The limit on output and hidden units is addressed to facilitate identification and evaluation by assigning the value 1 to the completed vector component X_p (N+1), which is denoted by the symbol N+1. The installations of the input and output units are linear. $net_p(j)$, the input to the Jth hidden unit, is stated [31] as follows:

$$net_p(j) = \sum_{k=1}^{N+1} W_{hi}(j, k) X_p(k) \quad 1 \leq j \leq N_h \quad (1)$$

With the output activation for the Pth training pattern, $O_p(j)$, is stated as follows:

$$O_p(j) = f(net_p(j)) \quad (2)$$

The sigmoid function is often selected as the non-linear activation:

$$f(net_p(j)) = \frac{1}{1 + e^{-net_p(j)}} \quad (3)$$

In equations (7) and (8), the N input units are denoted by the index K, whereas W_{hi} (J,K) represents the weight linking the Kth input to the Jth hidden unit.

The MLP's performance is assessed using the MSE formula:

$$E = \frac{1}{N} \sum_{p=1}^{Nv} E_p = \frac{1}{N} \sum_{p=1}^{Nv} \sum_{i=1}^M [t_p(i) - y_p(i)]^2 \quad (4)$$

Where:

$$E_p = \sum_{i=0}^M [t_p(i) - y_p(i)]^2 \quad (5)$$

E_p is the intended output for the P th pattern, and t_p relates to the error in the P th pattern. This also enables the napping error for the i th output unit to be calculated as follows:

$$E_i = \frac{1}{N_v} \sum_{p=1}^M [t_p(i) - y_p(i)]^2 \quad (6)$$

The i th output is represented as:

$$y_p(i) = \sum_{k=1}^{N+1} W_{oi}(i, k) X_p(k) + \sum_{j=1}^{N_h} W_{oi}(i, j) O_p(j) \quad (7)$$

In equation 13, $W_{oi}(i, k)$ indicates the weight from input units to output units and $W_{oi}(i, j)$ The weight from hidden units to output units.

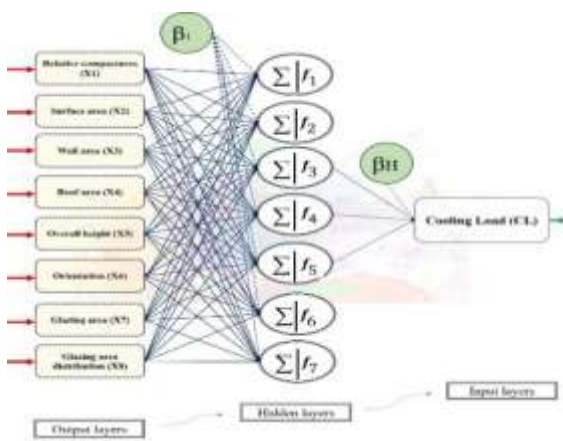


Figure 4: A multilayer perceptron

3.2. Biogeography-based optimization (BBO):

Whenever an environment is densely inhabited, several species will likely depart to surrounding environments, whereas few species will immigrate due to the unavailability of additional resources for migratory species. Similarly, whenever an environment is poorly inhabited, it contains few species. It is, therefore, eligible to secure many immigrants, but few species are inclined to depart due to their low numbers. Whether immigrants can thrive following migration is a separate concern; however, the new species' immigration may increase the biological richness of the environment and make it more suitable for existing species. In the 1990s, [35] this concept of the ecosystem as an optimizing system was first proposed. Biogeographers argue that a biogeography concept centered on maximizing the environment's state for biological activity is preferable to one based on homeostasis [36]. In reality, several instances of optimal solutions to biogeographical phenomena, such as

the Krakatoa island phenomenon [37] and the Amazon rainforest [36], corroborate this point of view.

With an alternative perspective, biogeography is sometimes seen as a procedure that maintains ecological balance. Throughout time, the opposing pressures of emigration and immigration culminate in an equilibrium of species' level diversity in a diverse habitat. Specifically, equilibrium is the point where the emigration and immigration curves intersect. In the 1960s, the equilibrium perspective in biogeography initially gained popularity as researchers challenged the equilibrium approach while increasingly adopting the optimality perspective.

Although biogeographical phenomena have been contested as an optimization procedure, suitable responses have been provided to address these issues. It must be emphasized that optimization and equilibrium are two separate viewpoints on the same biogeographic phenomena; yet, this discussion opens up several new avenues for study in BBO.

As its name suggests, BBO is a unique optimization technique built upon biogeography. The following section provides an in-depth description of the BBO methodology. Similar to how biology's mathematics prompted the creation of other biology-based optimization techniques, we can incorporate biogeographic elements into BBO to enhance its optimization efficiency. Among these are the impact of geographical location on migration rates, non-linear migration curves to best-fit nature (as will be presented in the paper), species swarms, prey/ predator interactions, the impact of differing species mobilities on directional momentum throughout the migration, rates of migration, and the impact of ecosystems area and isolation on migration rates.

Biogeography-based optimization: BBO

This section outlines the biogeography-based optimization method in broad terms. Assume we have a problem requiring improvement and a variety of potential solutions. A comparable environment with a high habitat suitability index (HSI) is an effective solution. According to biogeography, this refers to a suitable geographical region for biological organisms. HSI is an indicator of the quality of the solution provided by the environment in an optimization problem, also known as fitness. A wrong solution is comparable to a low HSI environment. Thus,

the variety of species a solution describes depends on its HSI. Solutions with a large HSI are more willing to exchange their characteristics with other solutions.

In contrast, solutions with a lower HSI are more inclined to accept features shared by other solutions. This innovative method for solving broad optimization issues is known as BBO. Like other evolutionary approaches, BBO consists of two key steps: information exchange (which is performed in BBO through migration) and mutation. Migration is a probabilistic operation that enhances a habitat (H_i). We leverage the migration rates of every environment based on the probability exchange characteristics across habitats. For each habitat (H_i), we utilize its immigration rate, λ_i to determine probabilistically whether one should immigrate or not. If immigration is chosen, the emigrating habitat H_j is chosen probabilistically depending on the emigration rate μ_j .

$$H_i(SIV) \leftarrow H_j(SIV) \quad (8)$$

An SIV is a suitability index parameter that indicates the livability of an island in biogeography. An SIV is a solution characteristic in BBO, analogous to a gene in GAs. The mutation is a probabilistic agent that arbitrarily adjusts the SIV of the habitat according to the prior probability of the environment's species count. The objective of mutation is typically to promote genetic diversity within a population. Mutation offers solutions with a poor HSI the opportunity to improve their performance. The mutation may make solutions with a high HSI even better than they currently are.

Two years later, [38] proposes modifying the migration operator for the case H_i . Given that in normal BBO, if $H_i(SIV)$ is chosen to be immigrated by $H_j(SIV)$, the operator $H_i(SIV)=H_j(SIV)$ is applied. This could reduce the search space, resulting in a locally optimal solution. Ma suggests a unique operator that combines the characteristics of immigrants and immigrant operators. This method enables BBO to preserve population variety and prevent local optima. In this strategy, $\alpha \in [0,1]$ is used to adjust the weights of the current candidate and immigration solutions. In [38], the authors investigate the setting of α experiment. The test results conclude that a proper value of α , say $\alpha = 0.5$, performs better than a large or a small value of α , say $\alpha = 0$ and 0.8 , respectively. In studies [39, 40] and [38], the migration operator is

designed to involve only one other solution, meaning that each candidate learns from a single peer during the migration process. To enhance this learning mechanism, Xiong [41] introduced a polyphyletic migration operator in 2004, which allows a candidate to learn from two different solutions simultaneously during each migration step. The corresponding pseudocode is presented in Algorithm 8, where $\varphi \in [0, 1]$ and $i, j, l, s \in [1, N]$. Here, N represents the population size, and D denotes the dimensionality of the problem. Following the migration step, Xiong [41] also incorporated an Orthogonal Learning Strategy (OLS), enabling the BBO algorithm to explore more promising solutions in the vicinity of current candidates.

Comparing other evolutionary approaches to BBO

BBO is a swarm-based, universal optimization technique that shares characteristics with other EAs, such as particle swarm optimization (PSO), evolutionary strategy (ES), differential evolution (DE), and ant colony optimization (ACO). For instance, they all use the same information-sharing operators. This makes BBO suitable for several issues when GAs and PSOs are employed. Nevertheless, BBO has characteristics that distinguish it from other EAs. Firstly, we observe that ES and GAs create offspring through crossovers; their solutions are lost at the end of each iteration, whereas the solutions of BBO are not lost but rather changed via migration. Secondly, we observe that ACO generates a new set of solutions for each iteration, whereas BBO maintains the same solution set across iterations. In contrast to PSO and DE, BBO solutions change immediately via migration, whereas PSO and DE change depending on the distinctions between these solutions. The benefits and drawbacks of BBO relative to other EAs require further research.

4. Results and discussion

This work evaluates the application of a meta-heuristic method, called BBO, in the advanced calculation of cooling demand in residential buildings. In this study, the process contributes to the solution by improving the CL estimation variables of an ANN by monitoring ambient factors. This section discusses the estimation outcomes of the MLP neural network instrument and the BBO-MLP ensembles. The suggested

BBO model's output has been displayed in tables and figures. For research, we have embraced the R and MATLAB programming languages. Conventional assessments of error measurements,

like R^2 and RMSE were used to evaluate the model's proposed performance. The cooling load efficiency of the proposed method is illustrated in Tables 1-3 and Figures 5-10.

Table 1. Network result variations based on the number in each hidden layer

| The number of neurons in each hidden layer | Network results | | | Scoring | | Total score | RANK | |
|--|-----------------------|-----------------------|----------------------|----------------------|-----------------------|----------------------|------|----|
| | RMSE _{total} | RMSE _{train} | RMSE _{test} | MSE _{total} | RMSE _{train} | RMSE _{test} | | |
| 1 | 1.155 | 1.206 | 1.170 | 5 | 5 | 5 | 15 | 6 |
| 2 | 0.702 | 0.694 | 0.700 | 8 | 8 | 8 | 24 | 3 |
| 3 | 0.686 | 0.673 | 0.682 | 9 | 9 | 9 | 27 | 2 |
| 4 | 0.732 | 0.745 | 0.736 | 7 | 7 | 7 | 21 | 4 |
| 5 | 1.673 | 1.688 | 1.677 | 4 | 4 | 4 | 12 | 7 |
| 6 | 2.413 | 2.371 | 2.400 | 2 | 2 | 2 | 6 | 9 |
| 7 | 0.599 | 0.609 | 0.602 | 10 | 10 | 10 | 30 | 1 |
| 8 | 0.800 | 0.799 | 0.800 | 6 | 6 | 6 | 18 | 5 |
| 9 | 1.829 | 1.793 | 1.818 | 3 | 3 | 3 | 9 | 8 |
| 10 | 3.050 | 2.917 | 3.011 | 1 | 1 | 1 | 3 | 10 |

4.1. Accuracy Indicators

To assess the forecasted CL, two statistical indices, namely, the coefficient of determination (R^2), and root mean square error (RMSE), were utilized to expand a color intensity ranking. It is worth noting that these evaluation criteria have been widely utilized in previous studies [42-44]. The formulations for RMSE and R^2 are presented in Equations (1) and (2), respectively.

$$RMSE = \sqrt{\frac{1}{U} \sum_{i=1}^U [(S_{i_{\text{observed}}} - S_{i_{\text{predicted}}})]^2} \quad (16)$$

$$R^2 = 1 - \frac{\sum_{i=1}^U (S_{i_{\text{predicted}}} - S_{i_{\text{observed}}})^2}{\sum_{i=1}^U (S_{i_{\text{observed}}} - \bar{S}_{\text{observed}})^2} \quad (17)$$

In the above equations, $S_{i_{\text{observed}}}$ and $S_{i_{\text{predicted}}}$ anticipate represent CL's real and expected values for the energy-efficient structure. U stands for the number and $\bar{S}_{\text{observed}}$ The mean of CL's real values. Machine learning models were constructed using an enhanced dataset in the Weka software environment. The outcomes of this procedure are provided in the following section.

4.2. Incorporated Optimizers and FIS

The BBO was presented with the equation of the calculated MLP as the primary challenge. Then, the cost function was calculated as the RMSE between the expected and actual CLs of the training specimens. The cost function is determined after each cycle to assess the simulation's validity. The BBO-MLP approach was then subjected to a sensitivity analysis dependent on the overall population. It is among the most significant variables of hybrid algorithms, as is pretty apparent. The networks are evaluated with ten swarm sizes ranging from 50 to 500 (50, 100, 150, 200, 250, 300, 350, 400, 450, and 500). Every network was constructed over 1000 cycles to reduce the error. As mentioned above, the approach yields ten convergence curves, as represented in Figure 5 for the BBO-MLP ensemble.

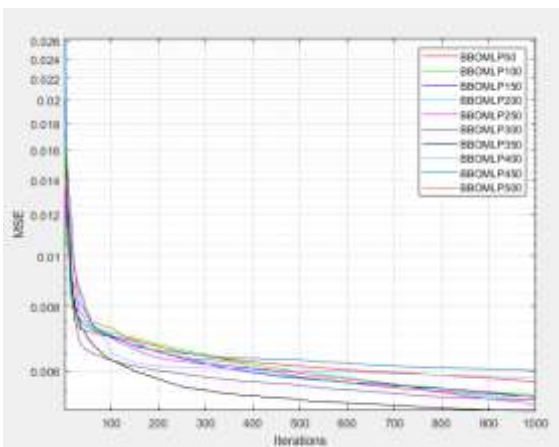


Figure 5: Finding the best-fit structure for BBOMLP 50-500

The best convergence curves (the lowest RMSE at the end of the procedure) are achieved for the swarm sizes of 400 for the BBO-MLP ensemble. Figure 6 shows the obtained RMSE values (3.509617617, 3.315078293, and 3.187975741) along with the alpha values (0.5, 0.6, 0.7, 0.8, 0.9, 1.0, 1.1, 1.2, 1.3, and 1.4) for a population size of 400. The lowest MSE shows the most accurate result and the best alpha value. According to this chart, the lowest MSE is obtained for $\alpha = 1.1$. As shown in Figure 6, the highest MSE is obtained for $\alpha=0.8$, indicating that this value of alpha yields less accurate results in predicting CL.

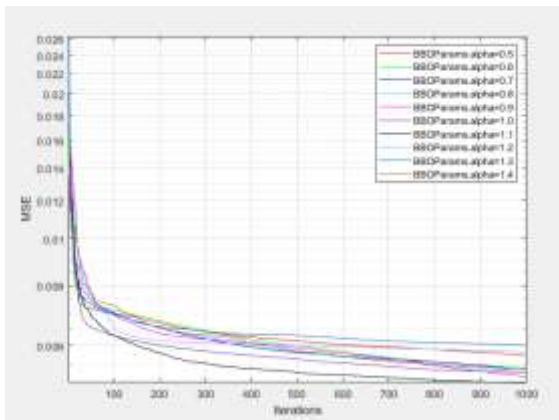
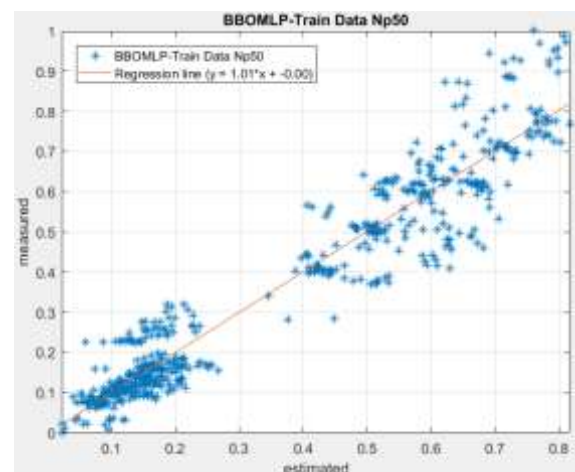


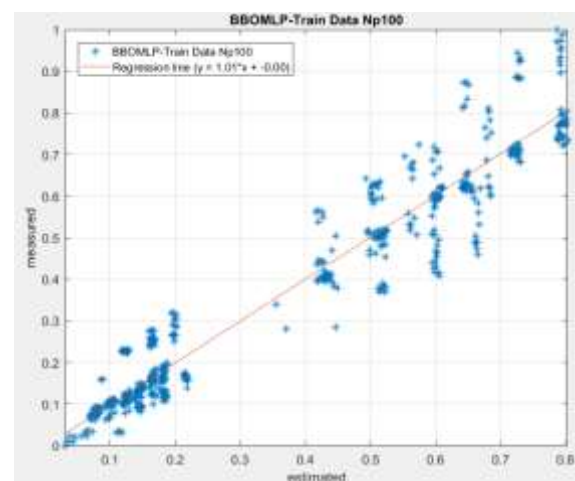
Figure 6: Best fit proposed 400 structures with various BBO alpha between 0.5 and 1.4

This section evaluates the precision of the created approaches by contrasting the expected and real CL amounts. Two error criteria, MAE and RMSE, were used to determine the performance error for both testing and training sets. The results' fitness in the testing and training stages shows the learning capacity and generalization ability, respectively. Concerning the testing stage, Figures 7 and 8 provide a graphical representation of the

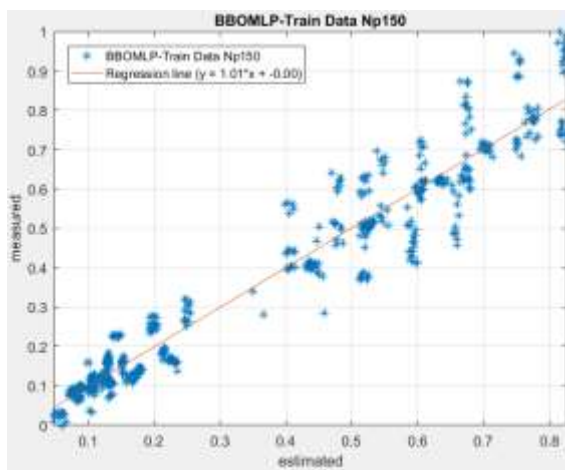
errors (the difference between the calculated and estimated CLs) and the correlation between the measured and expected CLs for each approach. There's no variance in the overall training performance. In other words, the greater the generalization power, the greater the comprehension in the training period. By taking the R^2 and the RMSE results from Figures 7 and 8, as shown in Table 2, can be obtained, which represent the combination of all regressions and rank the optimal size of the population. In addition, per Table 2, the R^2 amounts of 0.96007 and 0.9652 for testing and training, respectively, indicated that the population size of 400 was the most accurate.



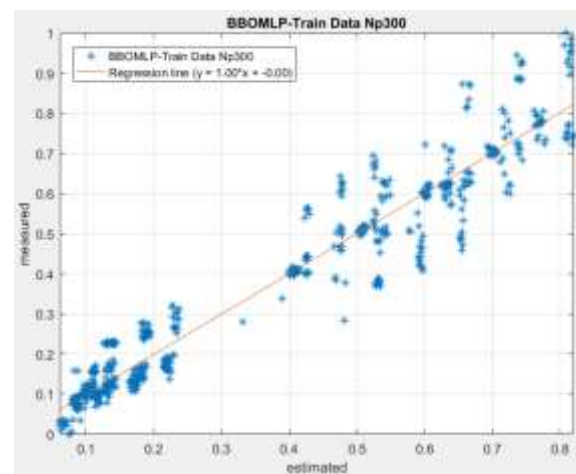
(a) BBOMLP train Np=50



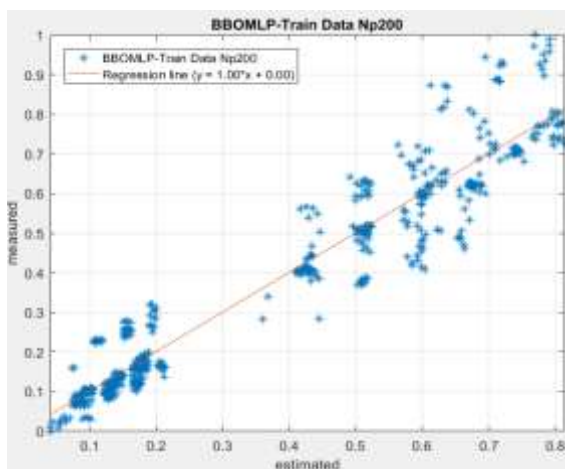
(b) BBOMLP train Np=100



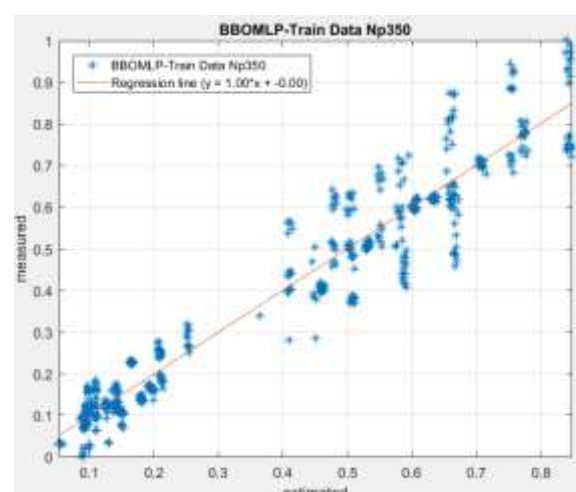
(c) BBOMLP train Np=150



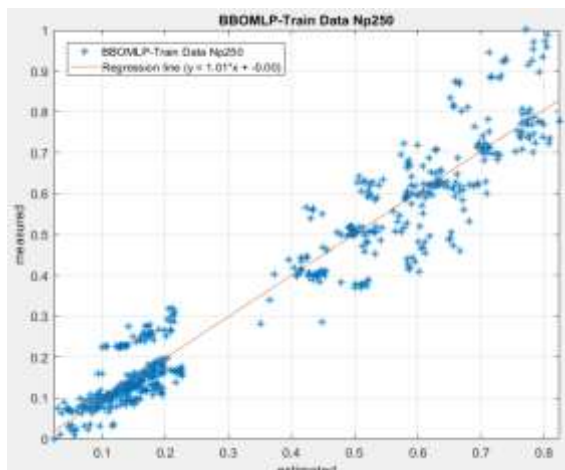
(f) BBOMLP train Np=300



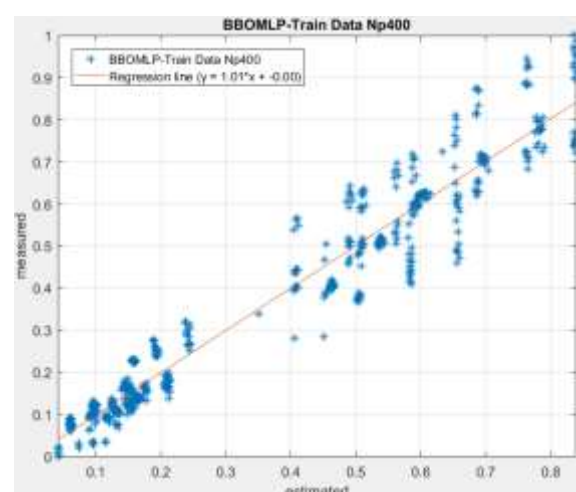
(d) BBOMLP train Np=200



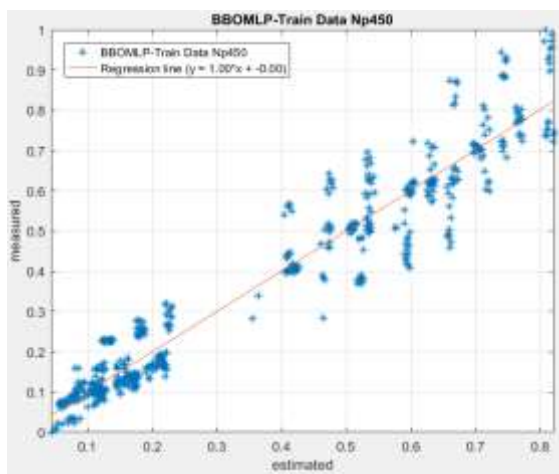
(g) BBOMLP train Np=350



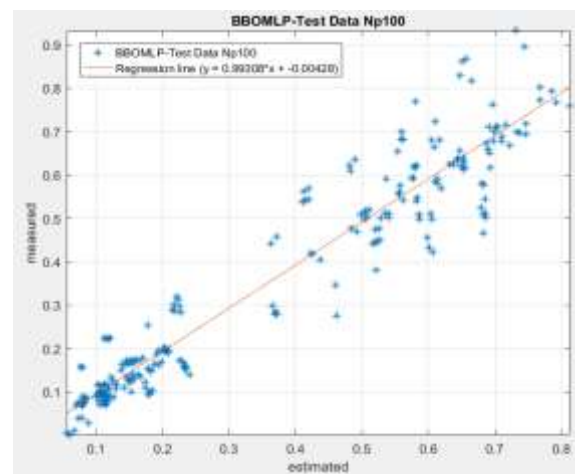
(e) BBOMLP train Np=250



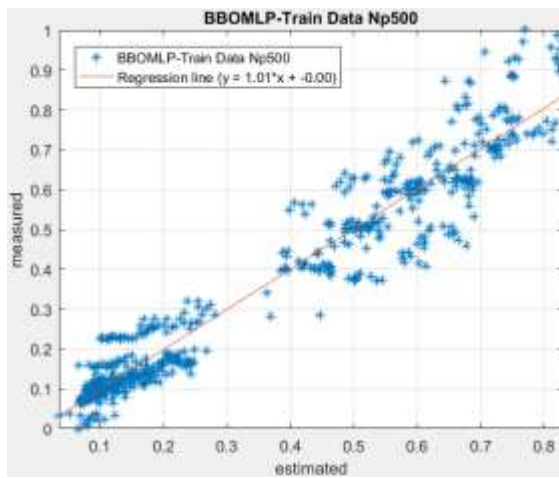
(h) BBOMLP train Np=400



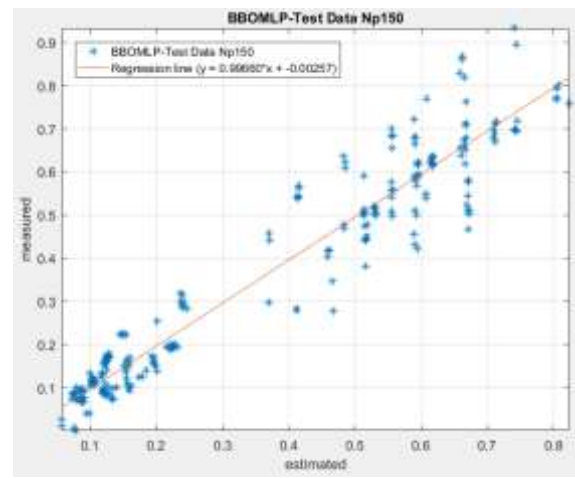
(i) BBOMLP train Np=450



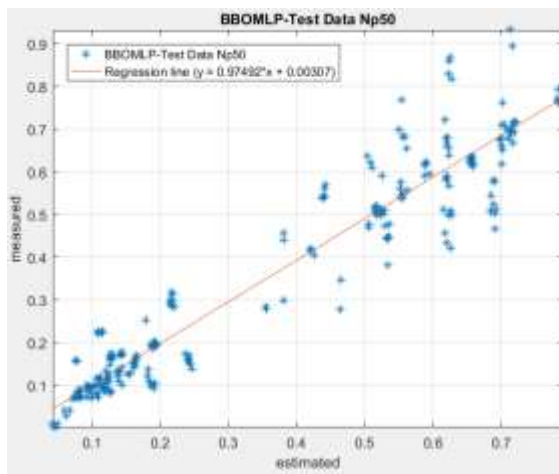
(b) BBOMLP train Np=100



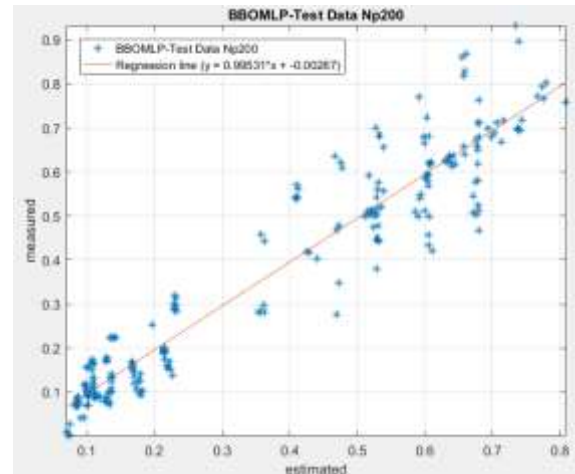
(j) BBOMLP train Np=500



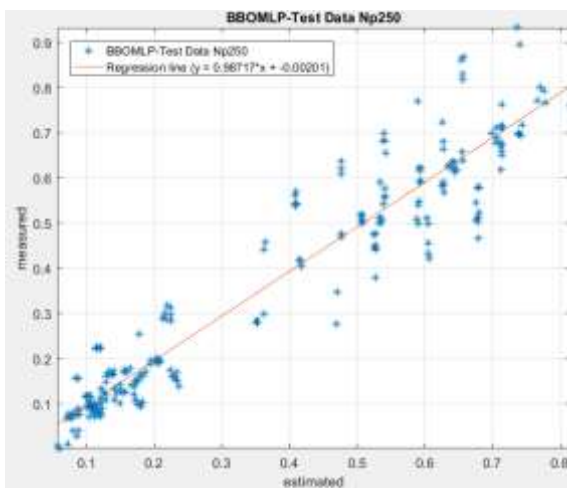
(c) BBOMLP train Np=150



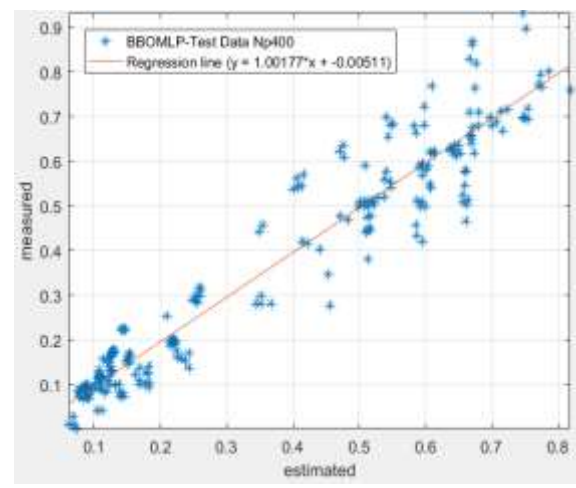
(a) BBOMLP train Np=50



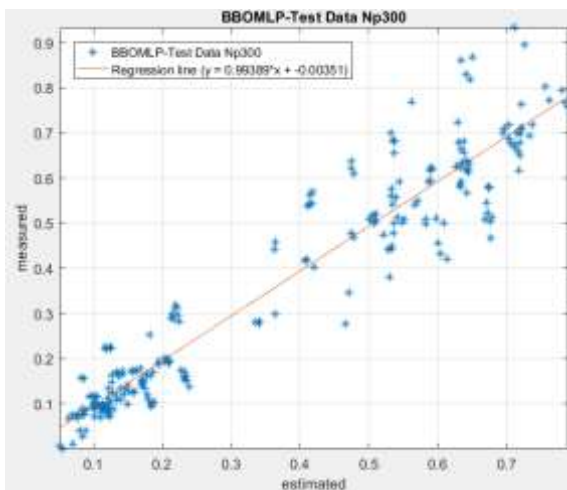
(d) BBOMLP train Np=200



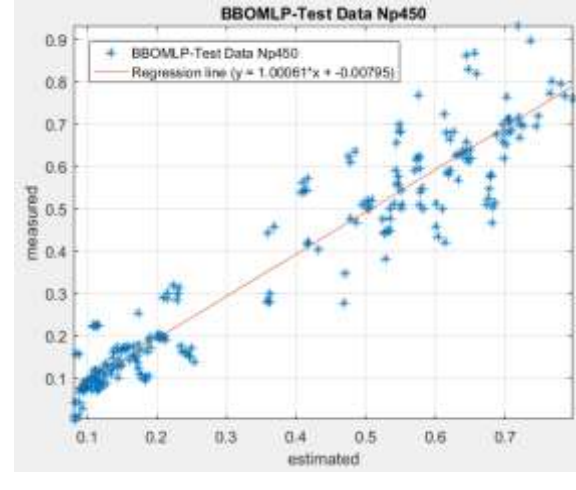
(e) BBOMLP train Np=250



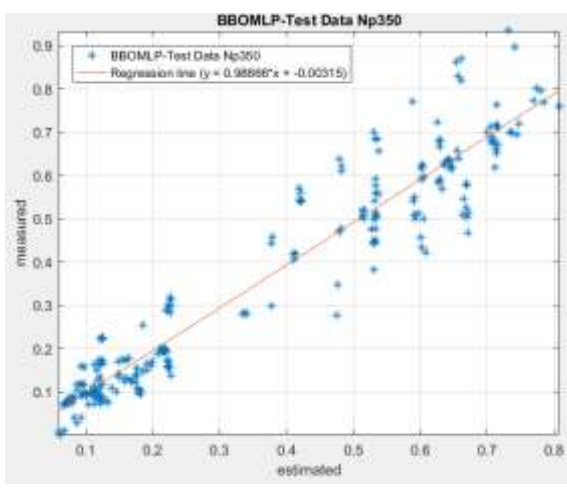
(h) BBOMLP train Np=400



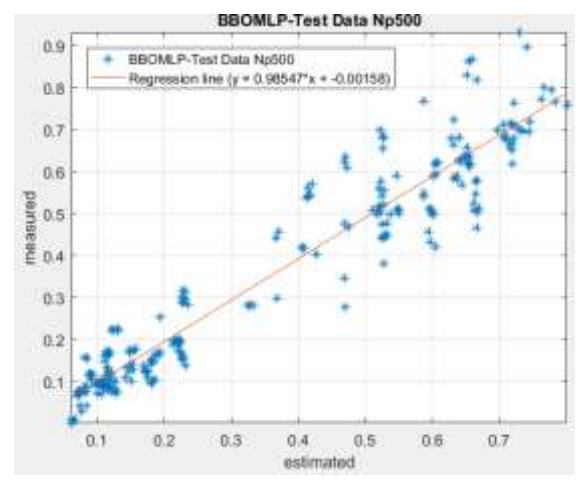
(f) BBOMLP train Np=300



(i) BBOMLP train Np=450



(g) BBOMLP train Np=350



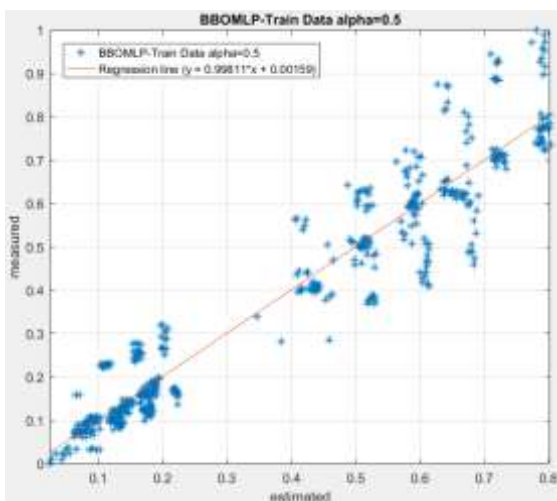
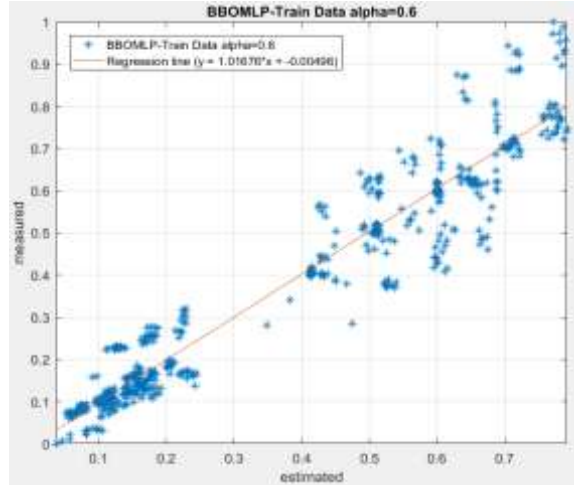
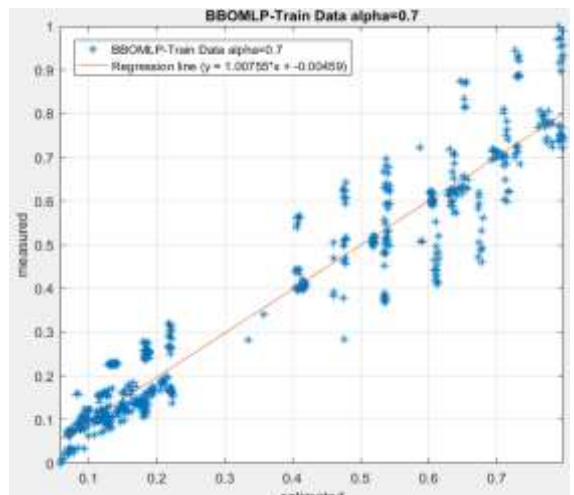
(j) BBOMLP train Np=500

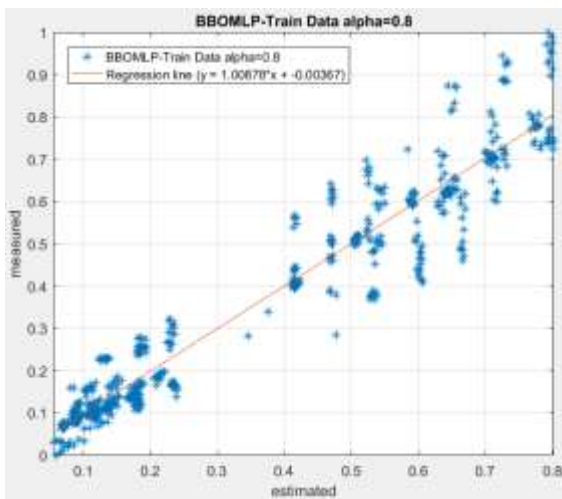
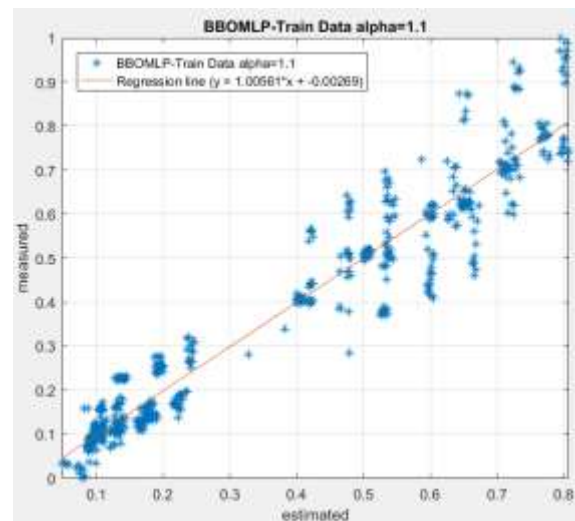
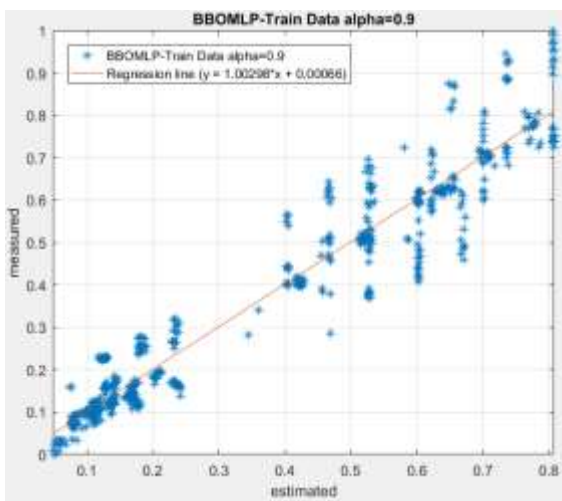
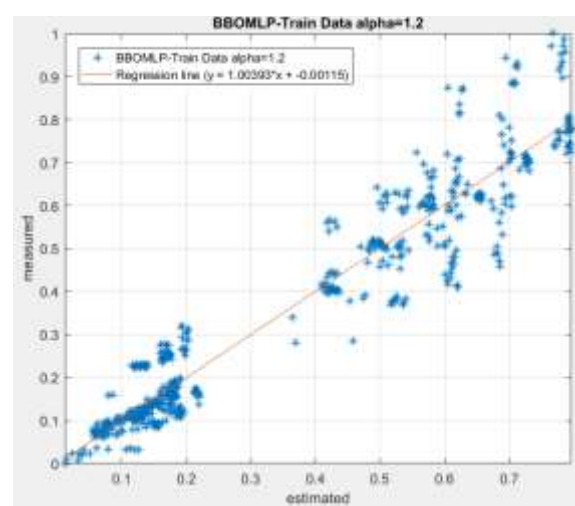
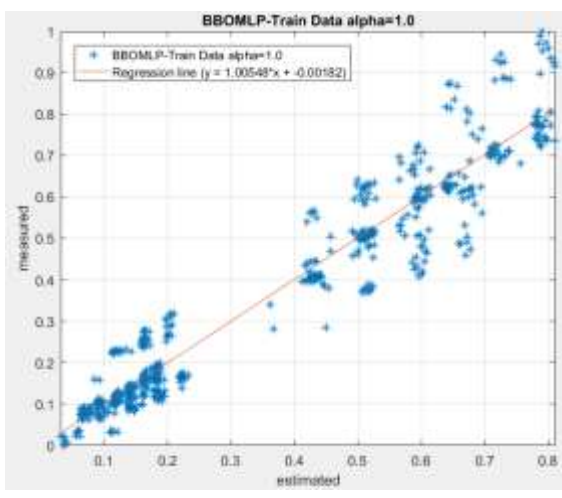
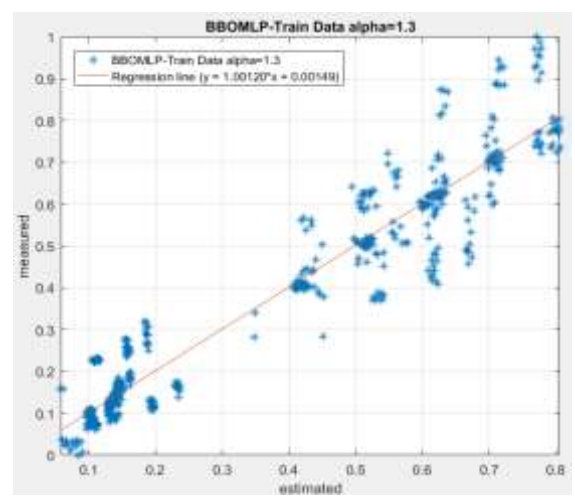
Figure 8: The precision of testing set performance of BBOMLP in the first optimization phase, after changing the population size between 50 and 500

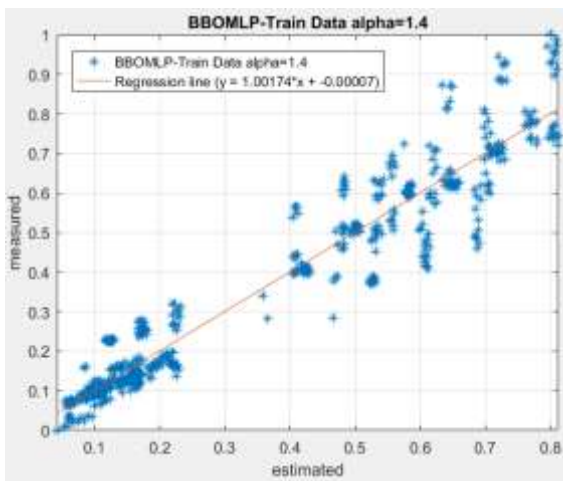
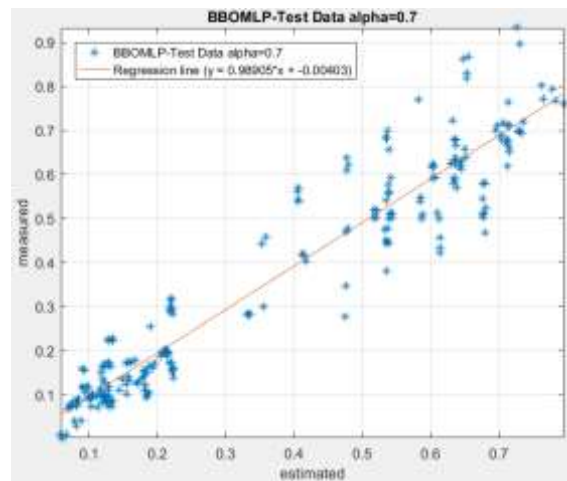
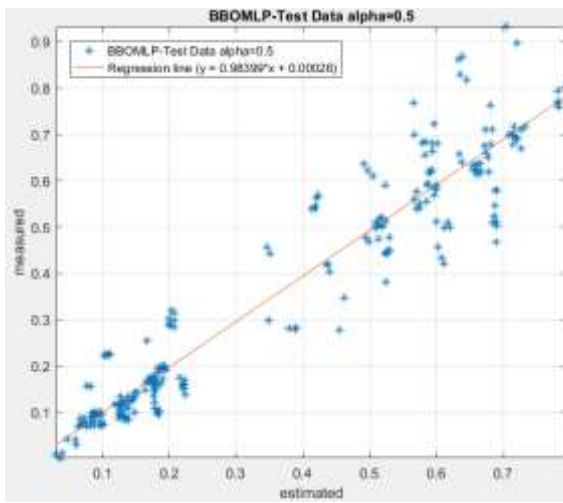
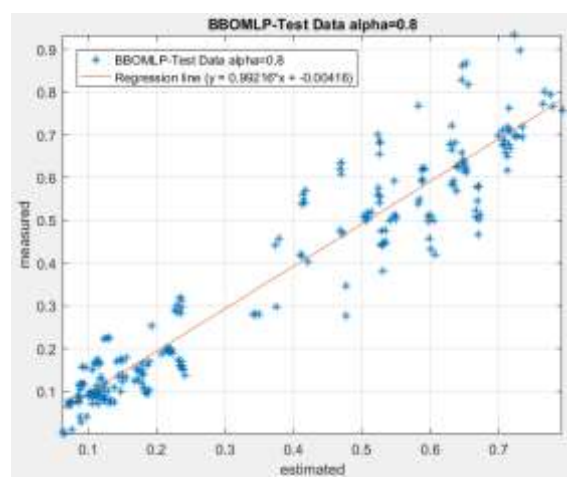
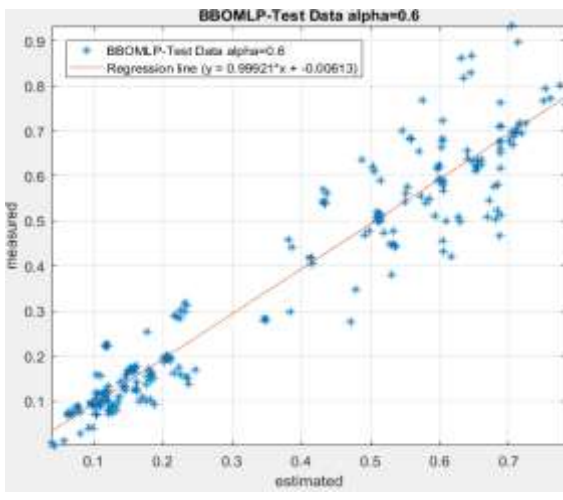
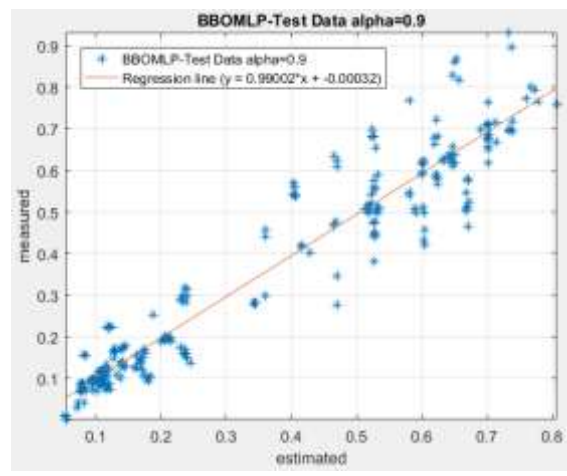
Table 2. The network outcomes for the BBOMLP having different swarm sizes

| Swam size | Training dataset | | Testing dataset | | Scoring | | | | Total Score | Rank |
|--------------|------------------|----------------|-----------------|----------------|----------|---------|----|----|-------------|------|
| | RMSE | R ² | RMSE | R ² | Training | Testing | | | | |
| 50 | 0.07573 | 0.95639 | 0.07564 | 0.95246 | 1 | 1 | 1 | 1 | 4 | 10 |
| 100 | 0.07186 | 0.96083 | 0.07262 | 0.95628 | 5 | 5 | 7 | 7 | 24 | 5 |
| 150 | 0.0689 | 0.96405 | 0.07011 | 0.95931 | 9 | 9 | 9 | 9 | 36 | 2 |
| 200 | 0.07179 | 0.9609 | 0.07368 | 0.95495 | 6 | 6 | 4 | 4 | 20 | 6 |
| 250 | 0.072 | 0.96067 | 0.07322 | 0.95553 | 4 | 4 | 5 | 5 | 18 | 7 |
| 300 | 0.0731 | 0.95943 | 0.07444 | 0.954 | 3 | 3 | 3 | 3 | 12 | 8 |
| 350 | 0.07082 | 0.96197 | 0.07214 | 0.95686 | 8 | 8 | 8 | 8 | 32 | 3 |
| 400 | 0.06773 | 0.96528 | 0.06946 | 0.96007 | 10 | 10 | 10 | 10 | 40 | 1 |
| 450 | 0.07367 | 0.95878 | 0.07445 | 0.95399 | 2 | 2 | 2 | 2 | 8 | 9 |
| 500 | 0.07116 | 0.9616 | 0.07279 | 0.95606 | 7 | 7 | 6 | 6 | 26 | 4 |

According to R² The value (i.e., the smallest RMSE at the end of the procedure) is acquired, indicating that a population size of 400 yields the highest accuracy outcome. Figures 9 and 10 illustrate the visual perspective of R² for testing and training stages for population size 400 and the alpha (0.5, 0.6, 0.7, 0.8, 0.9, 0.1, 1.1, 1.2, 1.3, and 1.4). As previously highlighted, Table 3 can be derived utilizing RMSE and R² amounts of Figures 9 and 10, since that is the sum of all regressions, and according to its ranking, the optimum alpha value is given. According to Figures 9 and 10, and Table 3, the maximum R² is found for alpha=1.2 (0.95574 and 0.95113 (for training and testing, respectively).

(a) BBOMLP train $\alpha=0.5$ (b) BBOMLP train $\alpha=0.6$ (c) BBOMLP train $\alpha=0.7$

(d) BBOMLP train $\alpha=0.8$ (g) BBOMLP train $\alpha=1.1$ (e) BBOMLP train $\alpha=0.9$ (h) BBOMLP train $\alpha=1.2$ (f) BBOMLP train $\alpha=1.0$ (i) BBOMLP train $\alpha=1.3$

(j) BBOMLP train $\alpha=1.4$ (c) BBOMLP test $\alpha=0.7$ (a) BBOMLP test $\alpha=0.5$ (d) BBOMLP test $\alpha=0.8$ (b) BBOMLP test $\alpha=0.6$ (e) BBOMLP test $\alpha=0.9$

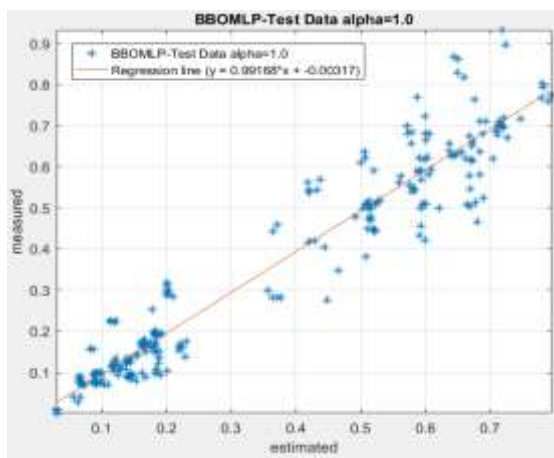
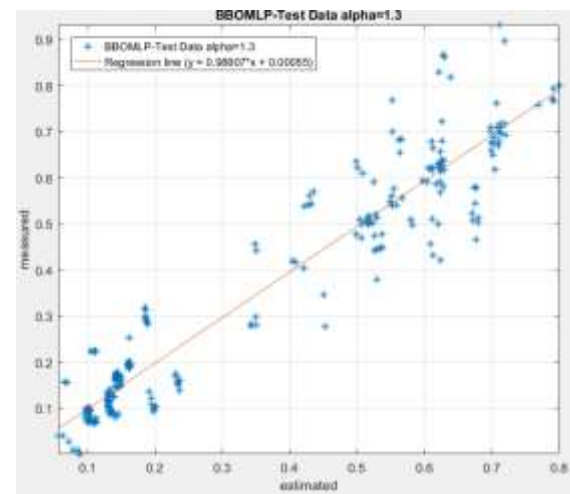
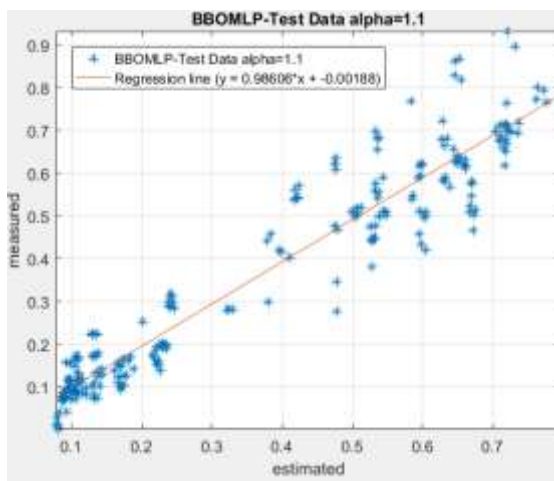
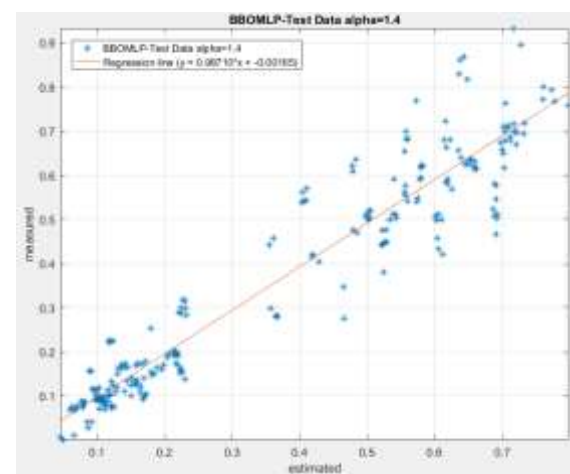
(f) BBOMLP test $\alpha=1.0$ (i) BBOMLP test $\alpha=1.3$ (g) BBOMLP test $\alpha=1.1$ (j) BBOMLP test $\alpha=1.4$

Figure 10: Testing accuracy for the proposed structure having different BBO alpha parameters varied from 0.5 to 1.4

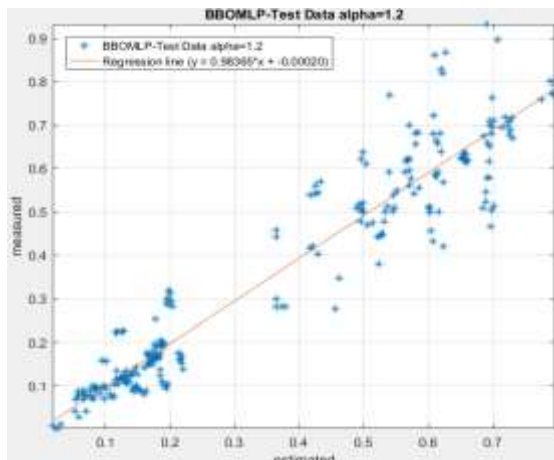
(h) BBOMLP test $\alpha=1.2$

Table 3. The network outcomes for the BBOMLP have a different alpha value

| Swam size | Training dataset | | Testing dataset | | Scoring | | | | Total Score | Rank |
|-----------|------------------|----------------|-----------------|----------------|----------|---------|----------|---------|-------------|------|
| | RMSE | R ² | RMSE | R ² | Training | Testing | Training | Testing | | |
| 0.5 | 0.0756 | 0.95655 | 0.07501 | 0.95328 | 3 | 3 | 3 | 3 | 12 | 3 |
| 0.6 | 0.07325 | 0.95927 | 0.07308 | 0.9557 | 4 | 4 | 8 | 8 | 24 | 6 |
| 0.7 | 0.07307 | 0.95946 | 0.07444 | 0.954 | 6 | 6 | 4 | 4 | 20 | 5 |
| 0.8 | 0.07263 | 0.95997 | 0.07444 | 0.954 | 8 | 8 | 4 | 4 | 24 | 6 |
| 0.9 | 0.07174 | 0.96095 | 0.07335 | 0.95536 | 9 | 9 | 7 | 7 | 32 | 8 |
| 1 | 0.07268 | 0.95991 | 0.07189 | 0.95717 | 7 | 7 | 10 | 10 | 34 | 9 |
| 1.1 | 0.07093 | 0.96185 | 0.07273 | 0.95614 | 10 | 10 | 9 | 9 | 38 | 10 |
| 1.2 | 0.07628 | 0.95574 | 0.07667 | 0.95113 | 2 | 2 | 1 | 1 | 6 | 1 |
| 1.3 | 0.07746 | 0.95433 | 0.07638 | 0.9515 | 1 | 1 | 2 | 2 | 6 | 1 |
| 1.4 | 0.07322 | 0.9593 | 0.07444 | 0.954 | 5 | 5 | 4 | 4 | 18 | 4 |

5. Discussion

It is evident from the preceding analysis and interpretation that numerous computations are required to assess the building power system, ranging from subsystem to building scales, and even regional and national scales. Each model has its own merits in specific usage scenarios. The engineering model has significant variances. The development of this model may involve several factors. It may be a very complex and exhaustive model, useful for precise computations.

On the contrary, by implementing proper simplification techniques, the model could be lightweight and simple to create while retaining its accuracy. Due to its high complexity and the lack of input information, implementing this comprehensive engineering model in reality is challenging, which is a well-acknowledged disadvantage. The statistical model is reasonably straightforward, but its shortcomings are readily apparent: inaccuracy and rigidity. ANNs are adept at addressing non-linear issues, making them very useful for estimating building energy consumption. It can produce accurate predictions if model selection and parameter setup are correctly completed. This approach has the drawbacks of requiring enough previous performance data and being quite sophisticated. The estimation of building energy usage has garnered significant interest from the academic community, yet many open, unresolved research topics remain. The following topics may be the subject of future study.

- Introduce novel prediction models that are more effective, stable, accurate, and efficient.
- Improve aspects of energy usage at the system level, evaluate possible models, and select the optimal model for each component.
- Apply energy forecasting to the Building Energy Management System (BEMS) for mutual advantage.
- Examine artificial intelligence models in various applications and improve prediction parameters.
- Evaluate each variable's impact on empirical models and balance the model performance and practicality in reality.
- Provide databases and gather accurate and adequate historical usage information from a multitude of situations for use in future studies.

This study demonstrated the effective use of an artificial neural network (ANN) model to address a critical energy-related challenge. Given the promising results, the proposed approach has the potential to be developed into a user-friendly platform, such as a graphical user interface (GUI), for early-stage prediction of cooling loads based on specific input parameters. Such a tool could be particularly valuable for engineers and architects aiming to optimize residential building designs, especially in terms of geometry and energy performance.

While several previous studies have successfully applied machine learning techniques to predict thermal loads in various building types, such as office, commercial, and industrial structures [45], further refinements could enhance the present method. First, comparing results based

on normalized data would help determine which data formats are most suitable for these simulations. Second, selecting an optimal number of input variables can simplify the model, reducing complexity and the number of parameters that require calibration. Additionally, linking HL with CL transforms the task into a multi-target prediction problem, which may increase complexity and should be weighed against its benefits.

Future research could also explore applying the model to a wider range of building types within a single study to improve its generalizability. Lastly, comparative studies are recommended to identify the most effective algorithms for integration with ANN or other intelligent systems.

The forecasting model proposed in this paper differed from previous studies in the analysis phases. Previous studies usually included just one phase of analysis. In this method, the analysis is conducted in the first phase, as in the previous work, and the optimal population size is selected. This swarm size has the lowest RMSE value and the most R^2 value and has the most accurate prediction. However, this section is the main difference between this work and the previous ones. In the second phase, the best swarm size of the first phase is examined. In this way, several different values for the alpha parameter (discussed in the previous section) have been considered, and the value that has the lowest RMS and the highest R^2 has been extracted.

5. Conclusions

Given the growing significance of conserving energy in modern human civilization, the primary objective of this study was to develop a unique hybrid approach for modeling the residential buildings' CL. The suggested approach imitates the herding behavior of BBO to enhance the neural network's efficiency. To do this, the BBO was fabricated with an MLP to produce the BBO-MLP ensemble. The CL was then predicted by considering eight relevant parameters. According to the estimated errors and the correlation of the findings, the BBO is effective at correcting the MLP's neural biases and weights. Based on the outcomes of the two presented statistical indices, namely, R^2 and RMSE, two statistical indices, were applied. The findings demonstrated that the proposed model (BBO-MLP) yields satisfactory estimation results in predicting CL in residential buildings. The values of R^2 in the BBO-MLP

model, which was obtained for a population size of 400, yielding 0.96007 and 0.96528 for the testing and training data sets, respectively. Additionally, in the case of RMSE, values of 0.06773 and 0.06943 were obtained from the training and testing datasets, respectively. Finally, by changing the alpha parameter's value for a population size of 400, the best accuracy results were obtained for alpha = 1.2. These results show the value of (0.95547 and 0.95113) for R^2 and (0.07628 and 0.07667) for the RMSE of the training and testing datasets, respectively.

6. References

- [1] Petroleum, British, BP statistical review of world energy June 2013, London: British Petroleum, (2013),
- [2] Xu, Xiaoqi, John E Taylor, Anna Laura Pisello, Patricia J Culligan, The impact of place-based affiliation networks on energy conservation: An holistic model that integrates the influence of buildings, residents and the neighborhood context, *Energy and buildings*, 55 (2012) 637-646,
- [3] Martínez-Molina, Antonio, Isabel Tort-Ausina, Soolyeon Cho, José-Luis Vivancos, Energy efficiency and thermal comfort in historic buildings: A review, *Renewable and Sustainable Energy Reviews*, 61 (2016) 70-85,
- [4] Kreider, JF, DE Claridge, P Curtiss, R Dodier, JS Haberl, M Krarti, Building energy use prediction and system identification using recurrent neural networks, (1995),
- [5] Efficiency, Energy, Buildings energy data book, US Department of Energy. <http://buildingsdatabook.eere.energy.gov/>. John Dieckmann is a director and Alissa Cooperman is a technologist in the Mechanical Systems Group of TIAX, Cambridge, Mass. James Brodrick, Ph. D., is a project manager with the Building Technologies Program, US Department of Energy, Washington, DC, (2009),
- [6] Thakar, Kush, Rajesh Patel, Gaurav Patel, Techno-economic analysis of district cooling system: A case study, *Journal of Cleaner Production*, 313 (2021) 127812, <https://doi.org/10.1016/j.jclepro.2021.127812>.
- [7] Sohani, Ali, Sahar Rezapour, Hoseyn Sayyaadi, Comprehensive performance evaluation and demands' sensitivity analysis of different optimum sizing strategies for a combined cooling, heating, and power system, *Journal of Cleaner Production*, 279 (2021) 123225, <https://doi.org/10.1016/j.jclepro.2020.123225>.
- [8] Akpan, Godwin Effiong, Usenobong Friday Akpan, Electricity consumption, carbon emissions and economic growth in Nigeria, *International Journal of Energy Economics and Policy*, 2 (2012) 292-306,
- [9] Chung, Min Hee, Eon Ku Rhee, Potential opportunities for energy conservation in existing

buildings on university campus: A field survey in Korea, *Energy and Buildings*, 78 (2014) 176-182,

[10] Gul, Mehreen S, Sandhya Patidar, Understanding the energy consumption and occupancy of a multi-purpose academic building, *Energy and Buildings*, 87 (2015) 155-165,

[11] Amiribesheli, Mohsen, Hamid Bouchachia, A tailored smart home for dementia care, *Journal of Ambient Intelligence and Humanized Computing*, 9 (2018) 1755-1782,

[12] Amiribesheli, Mohsen, Asma Benmansour, Abdelhamid Bouchachia, A review of smart homes in healthcare, *Journal of Ambient Intelligence and Humanized Computing*, 6 (2015) 495-517,

[13] Andreu, Javier, Plamen Angelov, An evolving machine learning method for human activity recognition systems, *Journal of Ambient Intelligence and Humanized Computing*, 4 (2013) 195-206,

[14] Zhang, Qiang, Zhe Tian, Yan Ding, Yakai Lu, Jide Niu, Development and evaluation of cooling load prediction models for a factory workshop, *Journal of Cleaner Production*, 230 (2019) 622-633, <https://doi.org/10.1016/j.jclepro.2019.05.085>.

[15] Yang, Liu, Haiyan Yan, Joseph C Lam, Thermal comfort and building energy consumption implications—a review, *Applied energy*, 115 (2014) 164-173,

[16] Li, Yan, Xiaofeng Li, Natural ventilation potential of high-rise residential buildings in northern China using coupling thermal and airflow simulations, *Building Simulation*, Springer, 2015, pp. 51-64.

[17] Deb, Chirag, Lee Siew Eang, Junjing Yang, Mattheos Santamouris, Forecasting diurnal cooling energy load for institutional buildings using Artificial Neural Networks, *Energy and Buildings*, 121 (2016) 284-297,

[18] Malkawi, Ali, Bin Yan, Yujiao Chen, Zheming Tong, Predicting thermal and energy performance of mixed-mode ventilation using an integrated simulation approach, *Building Simulation*, Springer, 2016, pp. 335-346.

[19] Lechtenböhmer, Stefan, Andreas Schüring, The potential for large-scale savings from insulating residential buildings in the EU, *Energy efficiency*, 4 (2011) 257-270,

[20] Agency, European Environment, Final energy consumption by sector and fuel, European Environment Agency Brussels, Belgium, 2015.

[21] Vakiloroaya, Vahid, Jafar Madadnia, Bijan Samali, Modelling and performance prediction of an integrated central cooling plant for HVAC energy efficiency improvement, *Building simulation*, Springer, 2013, pp. 127-138.

[22] Ahmad, Muhammad Waseem, Monjur Mourshed, Baris Yuce, Yacine Rezgui, Computational intelligence techniques for HVAC systems: A review, *Building Simulation*, Springer, 2016, pp. 359-398.

[23] Wang, Jiangjiang, Xiaoling Qi, Fukang Ren, Guoqing Zhang, Jiahao Wang, Optimal design of hybrid combined cooling, heating and power systems considering the uncertainties of load demands and renewable energy sources, *Journal of Cleaner Production*, 281 (2021) 125357, <https://doi.org/10.1016/j.jclepro.2020.125357>.

[24] Ozarisoy, B., Energy effectiveness of passive cooling design strategies to reduce the impact of long-term heatwaves on occupants' thermal comfort in Europe: Climate change and mitigation, *Journal of Cleaner Production*, 330 (2022) 129675, <https://doi.org/10.1016/j.jclepro.2021.129675>.

[25] Tsanas, Athanasios, Angeliki Xifara, Accurate quantitative estimation of energy performance of residential buildings using statistical machine learning tools, *Energy and buildings*, 49 (2012) 560-567,

[26] Khayatian, Fazel, Luca Sarto, Application of neural networks for evaluating energy performance certificates of residential buildings, *Energy and Buildings*, 125 (2016) 45-54,

[27] Yu, Jae-Hak, Han-Sung Lee, Young-Hee Im, Myung-Sup Kim, Dai-Hee Park, Real-time classification of Internet application traffic using a hierarchical multi-class SVM, *KSII Transactions on Internet and Information Systems (TIIS)*, 4 (2010) 859-876,

[28] Roy, Sanjiban Sekhar, Reetika Roy, Valentina E Balas, Estimating heating load in buildings using multivariate adaptive regression splines, extreme learning machine, a hybrid model of MARS and ELM, *Renewable and Sustainable Energy Reviews*, 82 (2018) 4256-4268,

[29] Roberts, Andrew, Andrew Marsh, ECOTECT: environmental prediction in architectural education, (2001),

[30] Chou, Jui-Sheng, Dac-Khuong Bui, Modeling heating and cooling loads by artificial intelligence for energy-efficient building design, *Energy and Buildings*, 82 (2014) 437-446,

[31] Delashmit, Walter H, Michael T Manry, Recent developments in multilayer perceptron neural networks, *Proceedings of the seventh Annual Memphis Area Engineering and Science Conference, MAESC*, 2005.

[32] Hornik, Kurt, Maxwell Stinchcombe, Halbert White, Multilayer feedforward networks are universal approximators, *Neural networks*, 2 (1989) 359-366,

[33] Hornik, Kurt, Maxwell Stinchcombe, Halbert White, Universal approximation of an unknown mapping and its derivatives using multilayer

feedforward networks, *Neural networks*, 3 (1990) 551-560,

[34] Cybenko, George, Approximation by superpositions of a sigmoidal function, *Mathematics of control, signals and systems*, 2 (1989) 303-314,

[35] Volk, Tyler, *Gaia's body: Toward a physiology of Earth*, Springer Science & Business Media, 2012.

[36] Kleidon, Axel, *Amazonian biogeography as a test for Gaia*, Scientists Debate Gaia, MIT Press, Cambridge, MA, (2004) 291-296,

[37] Whittaker, RJ, MB Bush, Dispersal and establishment of tropical forest assemblages, Krakatoa, Indonesia, Special publication... of the British Ecological Society, (1993),

[38] Zhao, Shi-Zheng, Ponnuthurai Nagaratnam Suganthan, Multi-objective evolutionary algorithm with ensemble of external archives, *International Journal of Innovative Computing, Information and Control*, 6 (2010) 1713-1726,

[39] Yao, Xin, Yong Liu, Guangming Lin, Evolutionary programming made faster, *IEEE Transactions on Evolutionary computation*, 3 (1999) 82-102,

[40] Dorigo, Marco, Vittorio Maniezzo, Alberto Colorni, Ant system: optimization by a colony of cooperating agents, *IEEE Transactions on Systems, Man, and Cybernetics, Part B (Cybernetics)*, 26 (1996) 29-41,

[41] Zhou, Zongzhao, Yew Soon Ong, Prasanth B Nair, Andy J Keane, Kai Yew Lum, Combining global and local surrogate models to accelerate evolutionary optimization, *IEEE Transactions on Systems, Man, and Cybernetics, Part C (Applications and Reviews)*, 37 (2006) 66-76,

[42] Moayedi, Hossein, Mohammad Mehrabi, Mansour Mosallanezhad, Ahmad Safuan A Rashid, Biswajeet Pradhan, Modification of landslide susceptibility mapping using optimized PSO-ANN technique, *Engineering with Computers*, 35 (2019) 967-984,

[43] Alnaqi, Abdulwahab A, Hossein Moayedi, Amin Shahsavari, Truong Khang Nguyen, Prediction of energetic performance of a building integrated photovoltaic/thermal system thorough artificial neural network and hybrid particle swarm optimization models, *Energy conversion and management*, 183 (2019) 137-148,

[44] Moayedi, Hossein, Mehdi Raftari, Abolhasan Sharifi, Wan Amizah Wan Jusoh, Ahmad Safuan A Rashid, Optimization of ANFIS with GA and PSO estimating α ratio in driven piles, *Engineering with Computers*, 36 (2020) 227-238, <https://doi.org/10.1007/s00366-018-00694-w>.

[45] Deng, Hengfang, David Fannon, Matthew J Eckelman, Predictive modeling for US commercial building energy use: A comparison of existing statistical and machine learning algorithms using CBECS microdata, *Energy and Buildings*, 163 (2018) 34-43,